Design and properties of FSW tools: a literature review

L. Dubourg [a], P. Dacheux [b]

[a] Aerospace Manufacturing Technology Centre, National Research Council Canada, 5145 avenue Decelles, Montréal, Québec, Canada, H3S 2S4
[b] Aluminium Technology Centre, National Research Council Canada, 501, Boul. de l'Université, Saguenay, Québec, Canada, G7H 8C3.

Abstract

For fifteen years, Friction Stir Welding (FSW) has increasingly attracted interest in both industry and academia for welding of aluminium alloys and other low melting temperature metals. The process involves a rotating tool consisting of a pin and a shoulder. The pin is being inserted between adjoining metal pieces. The heat generated by the tool friction brings the metal to a plastic-like state and the pin mixes the pieces together in a sound and homogenous joint. The main advantages of this process, speed, repeatability, no filler and no joint preparation, improved mechanical properties and low residual stress, have made FSW a beneficial method in marine, railway rolling stock, construction and aerospace industries. Applications in aluminium and copper are growing while FSW in titanium and other higher temperature materials are increasingly studied. These progresses are the consequence of the new FSW tool development and a better process understanding. Nevertheless, one of the most important challenges is still the design of the tool shoulder-pin system to assure a good quality weld and to reduce the loads during the process. Consequently, based on an extensive literature survey, a review is presented on FSW tools, covering the design, the properties and the applications. After a brief presentation on the interaction mechanisms between the tool and the metallic sample, the paper describes the typical tool designs and their characteristics. Finally, emerging tool geometries are reported.

1- Introduction

Friction stir welding (FSW) has quickly evolved since TWI has patented this technology in 1991. The heat generated mainly by the shoulder friction against the base metal brings the metal to a plastic-like state and the pin stirs the adjoining materials together in a sound and homogenous weld. Since melting seems to not be reached, FSW is considered as a solid-state welding process and it can be used in multiple positions and geometries [1, 2]. The main advantages of this process are the relative high welding speed compared with traditional GTAW or GMAW process, the high repeatability, the absence of fumes, shielding gas, filler material, joint preparation and ultraviolet radiation, the high mechanical properties of weldment, low residual stress level and distortion, the ability to weld aluminium alloys which cannot be fusion welded such as 2xxx or 7xxx series and the ability to weld dissimilar materials like Al to steel [1-6].

All these advantages have made the FSW process a beneficial welding method in marine, railway rolling stock, construction and aerospace industries [7]. Moreover, this friction technique can be applied to surface modification for different goals: processing for

superplasticity, casting modification, powder processing and metallic matrix nanocomposite elaboration [8]. The advantages of friction surface processing are the relative low amount of heat input, the extensive and controlled plastic flow, the very fine microstructure leading to the superplasticity behaviour of certain alloys (AA7075 [9], AA2024 [10]), the random misorientation of grain boundaries, the mechanical stirring of the surface layer and the large forging pressure.

Since the stirring tool is one of the process keys, its development drives the evolution of FSW process. This paper explores the parameters of tool design and their relation to heat generation, material flow and the formation of quality weld. Authors have voluntary limited this review to tools for low temperature and strength materials (aluminium, copper, magnesium, lead). PCBN and W-Re tools used for the welding of high temperature and strength materials (steel, titanium, superalloys) are not reported.

2. Fundamental principles of Friction Stir Welding

The two phenomena involved in FSW process are the heating by the tool friction on the material and the material flow due to the tool stirring. Experiments and numerical models are intensely used to improve the understanding of these phenomena. However, numerical approach gives access to phenomena difficult to estimate by experiment. Predictive simulations should take into account the following topics: coupled friction/heat generation, plastic flow and slip surface development and finally heat and material flow [5].

2.1 Heat generation

Although FSW energy input is about the same or smaller than arc welding [11], the heat is distributed over a wider zone by the shoulder contrary to a focused arc. Moreover, the intimate contact between the sample and the backing plate acts as a heat sink and dissipates efficiently the heat. Consequently, FSW is considered as a cold welding process leading to low residual stress level and distortion. Heat is mostly generated by the friction between the tool shoulder and the surface of the piece, followed by the high plastic work and the pin friction. Throughout literature, various percentage of the pin contribution to the heating process are available: 2% [1], 20% [1], 25% [12] and 51% [1]. However, a general trend adopts a contribution lower than 5%. The contribution of each component of the process (shoulder friction, pin friction and plastic work) on the heating is clearly underlined by Dong *et al.* for AA6061 T6 welding [13]. Fig. 1 shows the heat production due to friction alone (Fig. 1.a), plastic work alone (Fig. 1.b) and combined friction/plastic work (Fig. 1.c). In the case of friction alone, the temperature under the shoulder (about 350°C) is close to the one under the pin (300°C). However, this temperature is distributed on a larger surface, which causes a higher energy input. Moreover, the heating generated by the pin is close to the surface backing where the heat extraction is maximum. These two phenomena confirm the primary contribution of shoulder friction on the heat generation in the FSW process. In the case of plastic work alone (Fig. 1.b), the global temperature is relatively low (about 100°C under the tool) compared to friction heating (250°C), except under the pin where the strain is higher. This simulation confirms the main role of friction on the heating. Finally, when the two

phenomena are combined (Fig. 1.c), the global temperature under the tool is around 250°C with local hotter zones under the shoulder and the pin (>350°C).

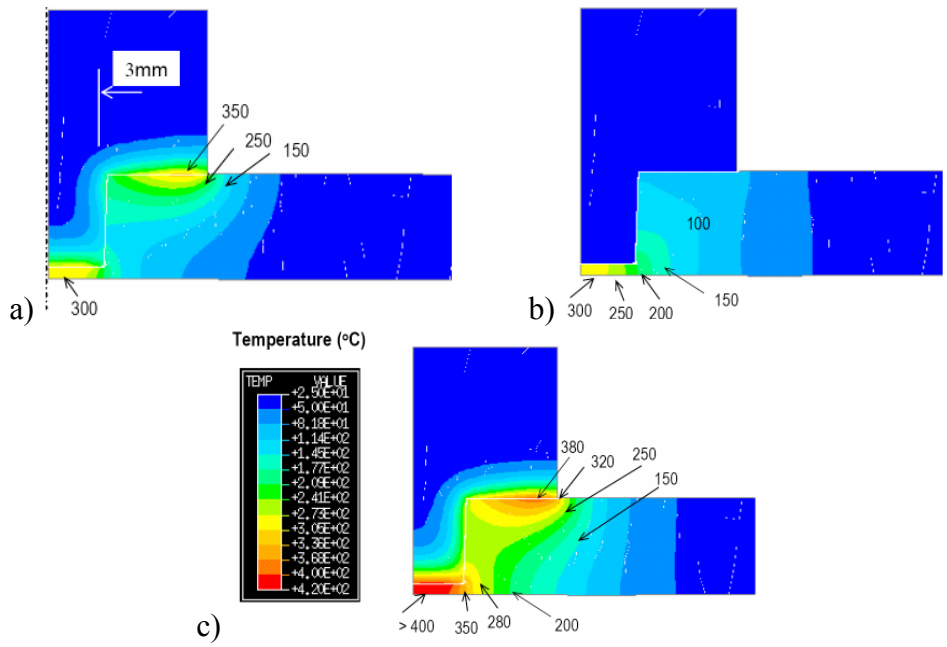

Figure 1: heat generation due to: a) tool friction, b) plastic work, c) tool friction and plastic work. Courtesy of Dong *et al.* [13].

The heat input by the shoulder friction may be calculated by Eq. 1 [14, 15]. As shown in this equation, the power input increases with the increase of friction coefficient, the forging force (i.e. the normal load acting by the tool), the rotational speed and the shoulder diameter.

$$q_0 = \frac{4}{3}\pi^2 \mu P N R^3$$

Equation 1: q_0: net power (W), μ: friction coefficient between the piece and the tool, P: pressure distribution (MPa), N: rotational speed (rpm), R: surface radius (mm).

The friction in front of the tool generates a plastic-like zone, which is then moved around the tool and deposited on the retreating side. This process is considered continuous along the workpiece. However, if melting occurs in front of the tool due to an excessive heating, less friction is generated due to the slip between the tool and the molten metal. As the temperature decreases, the material returns to a solid state and vice versa. This phenomenon may limit the use of high tool rotations and therefore the use of high welding speeds. Consequently, a material with a low melting point such as AA2024 (solidus temperature of 502ºC) cannot be welded as fast as AA5083 (solidus temperature of 574ºC). This is illustrated in Fig. 2, the AA2024 process window being smaller than the one of AA5083 [1, 16]. The melting point of different aluminium alloys in Fig. 2 can be used to sort the size of their process window (solidus temperature: 502ºC for AA2024, 477ºC for AA7075, 574ºC for AA5083 and 582ºC for AA6061). However, this correlation may be pondered by the high difference of mechanical properties and plastic flow between these aluminium alloys.

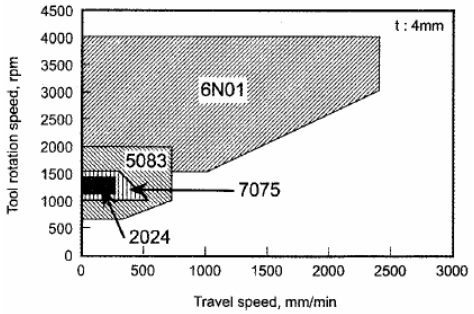

Fig. 2: process windows for several aluminium alloys. Solidus temperature: 502ºC for AA2024, 477ºC for AA7075, 574ºC for AA5083 and 582ºC for AA6061 [16].

This phenomenon of pin slippage may also explain the absence of molten pool during the FSW process. When the liquid state is reached, the process adjusts itself in order to return in a solid state welding. The local material melting in front of the tool may be confirmed by the presence of liquation in the thermo-mechanically affected zone (TMAZ) [17, 18]. Moreover, this phenomenon may explain the discrepancy between the numerical models of temperature (800ºC) and experiments (550ºC) observed by Colegrove and Shercliff [19]. However, the local melting is highly argued in the literature and no consensus is still adopted.

2.2 *Material Flow*

The complex flow around the FSW tool can be decomposed into three simpler flow components [20] *(i)* The first one may be considered as a cylinder of the welded material in rigid body rotation separated from the rest of the weld by a cylindrical shearing surface, i.e. a surface of velocity discontinuity (see Fig. 3.a). This rotating cylinder is conceived as attached to the FSW tool and its rotational speed is equal to that of the tool spindle. Its boundaries expand toward the tool shoulder to take into account the shoulder shape. Moreover, its thickness slightly increases on the retreating side to accommodate the metal transfer to the rear of the pin as the pin moves. In the case of thinner materials, this cylinder may be defined as a conical region to take into account the shorter pin length. The shearing surface is therefore located between the shoulder corner and the pin bottom (see Fig. 4 [13]). *(ii)* The second flow component is a homogeneous and isotropic flow field equal and opposite to the welding speed (see Fig. 3.b). This uniform translation is usually called “extrusion movement” by analogy to the same manufacturing process. *(iii)* The third component is a ring vortex flow encircling the tool and bringing metal up on the outside, in at the shoulder, down on the inside and out again on the lower regions of the pin (see Fig. 3.c). This flow is driven by the threads and/or flutes on the pin and can be reversed if the direction of the threads or the tool rotation is reversed. This vertical motion is clearly underlined by tracer experiments [21, 22]. In Schmidt *et al.*’s experiments [21], with 4 threads along the pin length, a marker is exposed to about 18 cycles around the pin. This generally leads to the disruptions and dispersion of the marker. As shown in Fig. 3.d, the combination of these three flows results in the formation of straight-through and vortex currents depending on the location. The material close to the advancing side travels in the rotating cylinder for a longer arc and is exposed to the axial flow of the ring vortex for a longer time. Consequently, the vortex current brings the metal to the bottom of the weld. Hence, vortex current residues are released to

the advancing side in order to conserve the material. On the other hand, the straight-through current occupies the retreating side as the metal in this region is exposed to the ring vortex for a short time. The relative amount of straight-through and vortex currents apparently fluctuates, perhaps due to an alteration in shear vs. friction slip on the shoulder surface [20]. These phenomena have been highlighted by Heurtier *et al.* [23, 24].

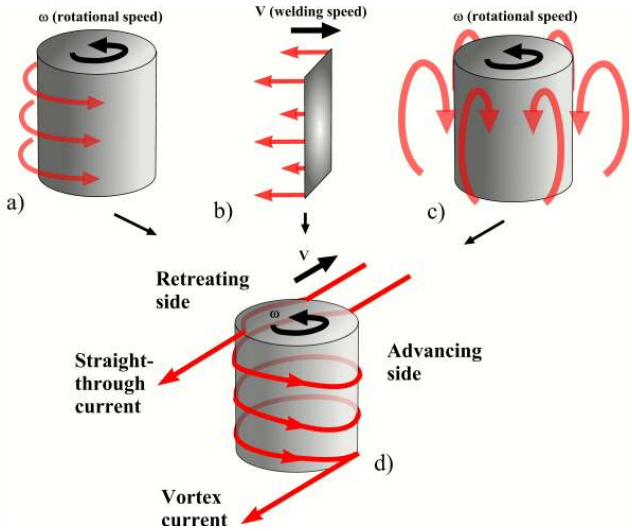

Fig. 3: Three incompressible flow fields: a) rigid body rotation, b) uniform translation, c) ring vortex, d) combination of the three flow fields.

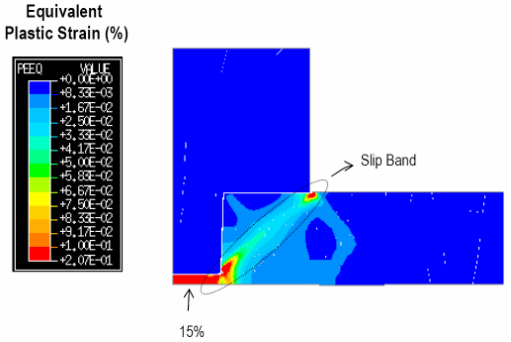

Fig. 4: Equivalent plastic strain during FSW process. Courtesy of Dong *et al.* [13]

Colegrove and Shercliff highlighted this complex metal flow by numerical simulation [19]. Fig. 4 shows in-plane velocity vectors of this simulation on horizontal planes at positions z = 0.1 mm (Fig. 5.a), 3.2 mm (Fig. 5.b, at mid-thickness) and 6 mm (Fig. 5.c, under the shoulder) from the bottom face. In all positions, a stagnation point is observed in the advancing side. The material close to this point is entrapped in the vortex current and flows around the pin. In the retreating side, straight-through currents are clearly underlined throughout the thickness. At mid-thickness (see Fig. 5.b), a large rotating region is observed around the tool, the solid line delineating the strain-rate equal to $2.s^{-1}$. This limits the cylinder in rigid body rotation illustrated in Fig. 3.a and approximates the boundary between the weld nugget and the TMAZ. Finally, Fig. 5.a shows the rotating material under the pin and it can be noted that the rotating tool above strongly influences the material flow in this region. This vortex flow, associated to the high temperature due to the extensive friction and metal work under the pin (see Fig. 1.c and Fig. 4), explains the complete welding of sheet root in the case of butt configuration. Indeed, the pin

length is generally smaller than the sheet thickness to avoid the wear or the breakdown of the pin on the backing.

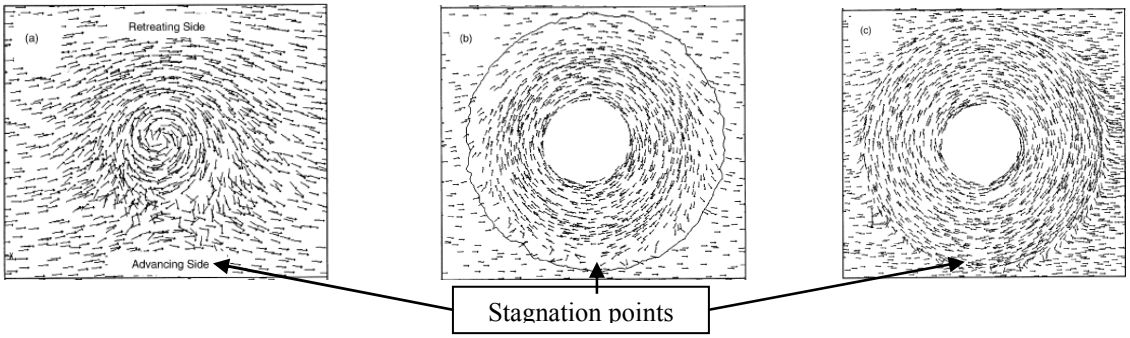

Fig. 5: in-plane velocity on horizontal planes at positions z = 0.1 mm (a), 3.2 mm (b) and 6 mm (c). Numerical simulation of AA5083 FSW. Courtesy of Colegrove *et al.* [19]

Dong *et al.* suggest a "boundary layer"' phenomenon in the stirring region [13]. This phenomenon may be quantified by the feed ratio *(k)* between the welding speed *(v)* and rotational speed *(ω)* (see Eq. 2).

$$k = \frac{v}{\omega}$$

Equation 2: (k) feed ratio (mm/tr), (v) welding speed (mm/s), (ω) rotational speed (tr/s).

The feed ratio measures the size of this boundary layer, which can be related to material flow properties under given temperature and pressure conditions, i.e. given FSW conditions. As shown in Fig. 6, a range of feed ratio *(k)* can be determined either experimentally [25] or numerically to obtain an acceptable weld quality under given welding conditions (material type, material thickness, tool shape).

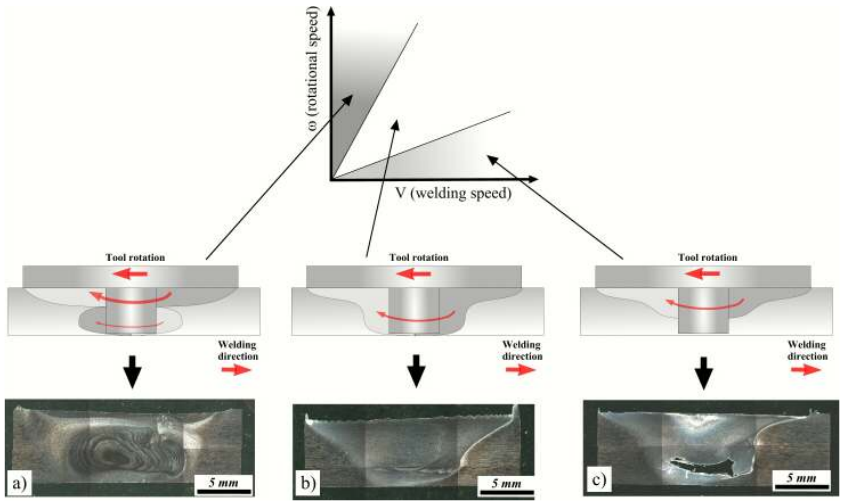

Fig. 6: Weld quality as function of feed ratio. FSW of AA6061, thickness of 8 mm [25].

For high *(k)* ratios (see Fig. 6.c), the minimum boundary layer for stable material flow may not be established leading to a lack of material feeding in the weld bottom, i.e. in the colder region. For low feed ratios (see Fig. 6.a), an overstirred situation may occur. In

this case, the rotational speed is high compared with the welding speed, causing a high heat generation and stirring under the shoulder. Consequently, the material in this zone may rotate more than in the weld bottom. This unstable condition causes the appearance of two nuggets and, in extreme conditions, the wormhole type defect. Between these limits, the flow boundary layer is stable, leading to a sound and free defect weld as shown in Fig. 6.b.

3. Tool Parameters

As seen in the previous chapter, the quality of FSWed joints are significantly affected by the welding parameters [26, 27]. The rotational speed of the shoulder-pin assembly, the welding speed, the downward forging force and finally the tool design must be optimized to obtain a sound and homogeneous weld [28]. This chapter attempts to summarize the different designs and tool parameters that can alter the characteristics of a FSW joint: shoulder diameter, pin size and shape (see Fig. 7).

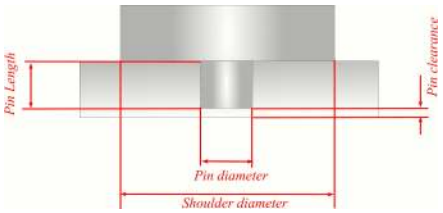

Fig. 7: Scheme of tool parameters

3.1 Shoulder diameter and shape

Shoulder size is the primary source of energy input (see Eq. 1). Since the heat input is a function of the shoulder radius to the third power and only linearly depends on the applied forge force and the rotational speed, the achievement of a sound weld is strongly dependent on the tool size [1, 29-31]. Moreover, Z-axis forge force is also a function of the shoulder radius [32]. Fig. 7 shows various shoulder diameters as a function of sheet thickness for 30 different set-ups reported in the literature (aluminium samples in butt configuration from 1 to 8.3-mm thick). A clear trend is observed: the shoulder diameter is about 2.3 times the sample thickness plus a constant of 7 mm. When the thickness increases, more energy input is necessary, this is obtained by the design of a bigger shoulder. However, Reynolds and Tang [32] observed that essentially equivalent welds may be made using a range of tool geometry, proving that the FSW process is relatively robust. Fig. 7 may also confirm that: for a given sample thickness, the range of shoulder diameters may be high. In the case of a smaller shoulder, the reduction in heat generation is balanced by a higher rotational speed.

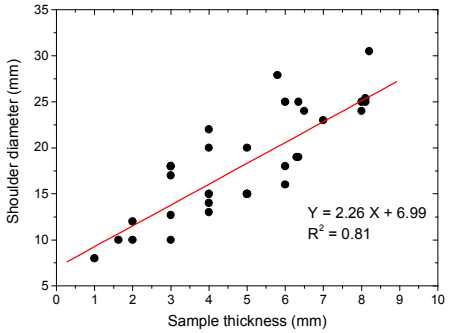

Fig. 7: Used shoulder diameter as a function of sample thickness for 30 different set-ups in the literature (range of thickness from 1 to 8.3mm, aluminium samples in butt configuration).

Two different shoulder shapes emerge from the literature: the scroll type and the cup type. The first one seems to be preferred for the larger tools and the cup shape for finer tools due to machining simplicity. The scroll shape is placed in the opposite direction of the tool rotation drawing the surface material towards the threaded pin where it is forced downward along the pin surface. This profile improves the surface finish, reduces the extruded flash and allows the tool to remain normal to the workpiece surface [33]. Some studies have reported that the stress corrosion crack propagation rate is much slower in FSWed substrates where the scroll shoulder is used [1, 34]. By using a small roll angle (2-3º), the cup shape increases the forging force for a same shoulder plunge, i.e. the same forge position [25]. This phenomenon leads to a higher forging and hydrostatic pressure, which may promote the material stirring and the nugget integrity.

3.2 Pin size and shape

Figure 8 shows the pin diameter and the pin clearance as a function of sheet thickness for 28 different set-ups reported in the literature. A general tendency, observed in Fig. 8.a, is that the pin diameter is approximatively equal to the sheet thickness for thickness from 1 to 8.3 mm. Moreover, the minimum pin diameter is about 3 mm. Again, the range of the pin diameters may be high. For example, for 8-mm thick plate welding, pin diameters from 8 to 13 mm leads to defect-free welds. Reynolds *et al.* examined the influence of pin diameters from 8 to 12 mm on the X-axis force (i.e. along the welding direction) and the specific weld energy [32]. For this range of tool geometries, pin diameter did not appear to influence the required x-axis force and the specific weld energy.

Fig. 8.b shows the pin clearance, i.e. the difference between the pin length and the sheet thickness (defined in Fig. 7). This value does not take into account the tool plunge during the process. This clearance is important to secure sufficient plastic deformation in the root of the weld. A pin clearance of 0 to 0.5 mm for thickness range of 1 to 8.3 mm has been reported in the literature (see Fig. 8.b), all these values leading to full penetrated welds. If the clearance is too small, this generates an unbonded area in the root and an early fracture during tensile or bend deformation will appear [25, 34]. It should be noticed that a null value of pin clearance is generally avoided as it may cause pin damage due to the tool plunge during the welding.

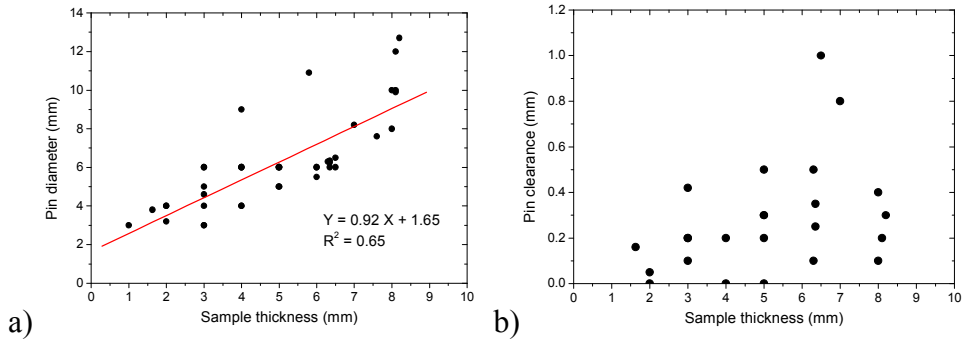

a) b)

Fig. 8: Used pin diameter (a) and pin clearance (b) as a function of sample thickness for different set-ups in the literature (range of thickness from 1 to 8.3 mm, aluminium samples in butt configuration).

An important parameter in FSW tool design is the ratio of dynamic volume (volume swept by the pin during rotation) to static volume (volume of the pin itself). Increasing this ratio results in a reduction in the formation of voids in the welds and allows the

surface oxide to be more effectively disrupted and dispersed within the microstructure [34, 35]. In conventional FSW, the dynamic/static ratio can be increased via the use of re-entrant features, flutes, threads and/or flats machined into the pin [12, 35, 36]. The presence of flats on the pin acts as the cutting edge of a cutter. Thereafter, the material is trapped in the flats and released behind the tool promoting thorough mixing. The extreme extension of this principle is the friction skew stir technique (see 4.2).

Exploitation of the dynamic/static ratio may be highlighted by the footprint technique. The polar plot of the force footprint shows the force vector experienced by the tool during each revolution (see Fig. 9).

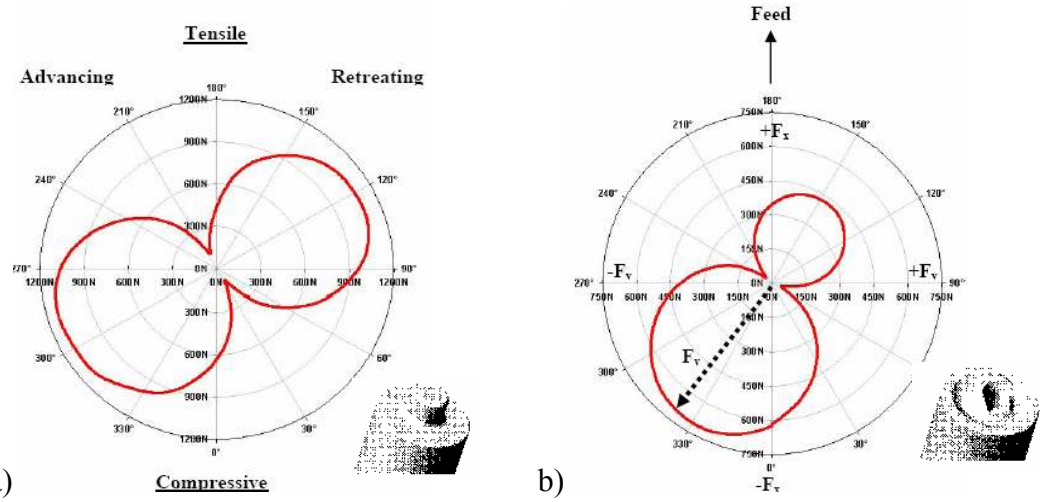

Fig. 9: Polar force plot for a spindle speed of 300 rpm and welding speed of 120 mm/min: a) non-profile tool, b) profile tool. Courtesy of Hattingh *et al.* [37].

Changes to tool geometry influence the polar plots and the relative areas of the lobe. Using such information and the total area of the plot helps in optimizing tool design. The area of such a plot is indeed related to the mechanical energy input [37]. For cylindrical tool geometry, the bi-lobed plot remains largely symmetrical although showing a slight expansion of the lobe on the advancing side of the weld (see Fig. 9.a). In the specific example given in Fig. 9.a, the high forces (Fy = 1050 N) on the tool are an indication of the poor suitability of this tool shape to stirring the weld metal. This tool has a forging action rather than a stirring action. Fig. 9.b shows the force footprint for a truncated and threaded tool with the same process parameters. In this case, the position of the strain is coincident with the truncated cut-out on the pin. The maximum forces are significantly lower than those obtained for the case of the non-profiled tool. The peak force, Fx, ahead of the tool is reduced to around 360 N while at the trailing edge the force is 615 N. Relatively low lateral forces Fy are reduced to 200 N and 400 N at 90° and 270° positions respectively. This clear reduction of the welding forces decreases the tool wear and the requirement of plate clamping restraints [37].

For a constant dynamic/static ratio, Colegrove and Shercliff have numerically demonstrated the major contribution of pin shape on the welding forces [38]. The profiles used for this study are shown in Fig. 10. All the tool shapes have a cross-sectional area of 121 mm^2 and a dynamic/static ratio of 1.15. The only exception is tool #4 where the

dynamic/static ratio is 1. The first three profiles compare the effect of flat (tool 1), concave (tool 2) and convex (tool 3) features on the tool. Following these experiments, authors observed that the axial force (i.e. the force along the welding direction) exerted on the pin is a consequence of two effects. *(i)* The amount of stirring that the profile induces around the tool. The greater the stirring, the lower the force required to push the tool through the material. Tools 1 to 3 indeed lead to a force up to three times lower than tool 4. *(ii)* The amount of the material trapped in the features of the profile. Such entrapment increases the axial force of the tool through the weld joint. Depending on processing conditions, the axial forces are 1500 kN/m for tool 1, 1800 kN/m for tool 2 and 800 kN/m for tool 3. This effect is particularly significant on the advancing side where shearing occurs within the trapped material, which is moving in an opposite direction to the flow. A profile as the one on tool 3 that enables material to slip across the tool surface avoids this shearing force effect, lowering the traversing force. Consequently, the convex tool 3 that promotes material slip, while maintaining the tool ability to stir the material with a high dynamic/static ratio compared to tool 1, minimises the traversing force [38].

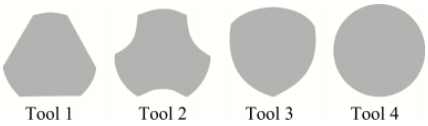

Fig. 10: Tool profiles examined in [38]

The effects of pin angle (see Fig. 11) on the FSW process were investigated by Buffa *et al.* with a thermo-mechanical fully coupled 3D FEM analysis [39, 40]. The authors observed that the temperature in the nugget, the HAZ and the TMAZ increases with the pin angle from 0º to 40º. This was mainly ascribed both to the increase in friction heat due to the larger contact area between the welding pin and workpiece and to the increase of plastic work deformation energy. Large pin angle promotes also high hydrostatic pressure in the weld zone, which is significantly important for enhanced nugget integrity. However, the high temperature and hydrostatic pressure may also favour severe tool wear. Finally, as shown in Fig. 11, the conical pin produces a helical movement in the nugget due to the vertical force component. Fig. 11 a-f shows the material flow patterns at different pin angle (Fig. 11.a for 0º, Fig. 11.b for 30º and Fig. 11.c for 40º), the arrows representing the material velocity vectors. A small vertical material flows are observed with a cylindrical pin (see Fig. 11.a). On the contrary, conical pin causes an additional down flow pattern, which becomes more remarkable as pin angle increases (see Fig. 11.b and c). Moreover, a helical movement is produced by the conical pin due to the circular movement components in the horizontal (x–y) plane (see Fig. 11.d) and in vertical (y–z) plane (see Fig. 11.e and f). This movement causes material to flow down in the advancing side and to flow up in the retreating side [40]. This property may be interesting in order to increase the ring vortex effect (see Fig. 3.c) of thread and flute features.

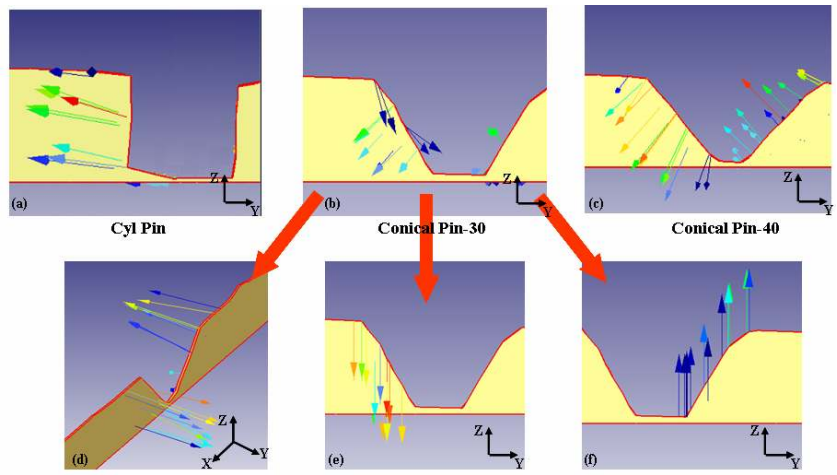

Fig. 11: Material flow patterns in weld zone at different pin angles (Vf = 100 mm/min). Courtesy of [40].

3.3 Threaded and flute type pin

If threads are right-hand and rotation is counter clockwise, the material is drawn down by the threads along the pin surface. Material may circulate multiple times around the tool before being deposited behind the tool. This phenomenon promotes material stirring, void closure and oxide breakdown. This configuration is the most used as the right-hand thread in a clockwise rotation results in poor quality weld [41]. Flutes can be considered as large threads. In fact, this geometry produces the same effect as pushing the material vertically [1]. Colegrove and Shercliff [12, 38] identified this behaviour by using computational fluid dynamics code to compare a tool with three flutes (see Fig. 12.a) with a tool with three flats (see Fig. 12.c). The main difference between the two shapes is the vertical movement of the material (see Fig. 12.b). The tool with three flutes traps the material in the flutes downwards [38].

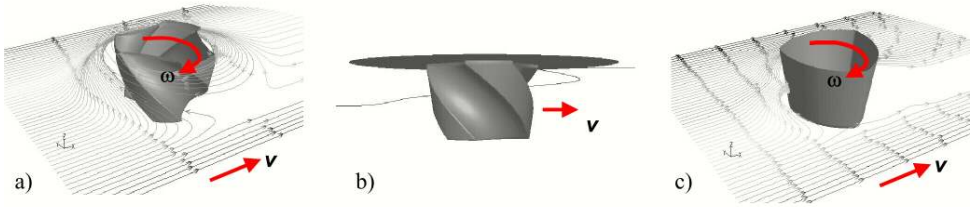

Fig. 12: Steamlines for isothermal: a) tool with three flats, b) tool with three flutes, c) single streamline for the tool with three flutes showing vertical movement. Courtesy of Colegrove and Shercliff [38].

4. Case studies

A number of tools have been developed during the last 15 years and used to join different materials, component thickness and joint types [42]. For the welding of thin sheets (< 12 mm), the most used tools are the cylindrical threaded pin and the Trivex ^{TM} due to their relative simple shape to machine on the short pin. For thicker materials (> 12 mm), the Triflute ^{TM} and Whorl ^{TM} are generally chosen. For lap joint, the most used tools are the Flared-Triflute ^{TM}, Skew ^{TM} and the whisk types.

4.1 Butt joint configuration

The classic FSW tool shape is the cylindrical or conical threaded pin as shown in Fig. 13. Triflute ™ (Fig. 14.a and Fig. 14.b) was developed from the Whorl ™ (Fig. 14.c) geometry, three flutes being added [29]. This tool is designed to provide enhanced flow and adequate stirring action, and thereby reduces or eliminates the presence of voids. Moreover, this geometry reduces the torque required to rotate the tool and the travel force during welding [29]. The pins of these tools were shaped as a frustum that displaces less volume than a cylindrical tool of the same root diameter.

a)  b) 

Fig. 13: a) cylindrical partially threaded pin tool, b) conical threaded pin tool with 3 flats. The 2 tools have a cup-shape shoulder.

a) 

b) 

c) 

Fig. 14: a) b) Triflute pins ™, c) Whorl ™ pin.

Fig. 15 shows the Trivex ™ tool and the MX Trivex ™ tool. As previously mentioned, the convex shape promotes material slip, while maintaining the tool ability to stir the material, and minimises the axial force. The Trivex ™ tool has a marginally lower traversing force than the MX Trivex ™ tool. This may be a consequence of the threads increasing the area carrying the limiting shear stress, which increases the traversing force for this shape [38].

a)  b) 

Fig. 15: a) Trivex ™ tool, b) MX Trivex ™ tool.

Shindo *et al.* [43] and Prado *et al.* [44] reported on the tool shape optimization for FSW of aluminum base MMCs (20% SiC reinforcement for [43] and 20% Al_2O_3 reinforcement for [44]). In these high strength materials with abrasive particles, the wear consumes the threads and leads to a slightly curved shape pin as shown in Fig. 16. However, with the use of the optimized shape (see Fig. 16 at 3.96 m), the tool does not wear out and produces homogenous and sound welds even in the absence of threads [43]. These observations suggest that shape-related solid-state flow control is an essential feature of FSW, especially in assuring limited tool wear and long tool life. Even in the case of very hard MMC, FSW can afford essentially little or no tool consumption when tool shape is optimized [44].

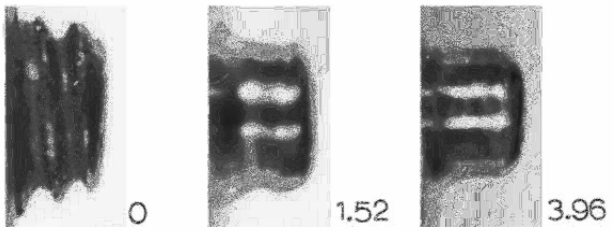

Figure 16: sequence showing pin wear during Al359-20% SiC MMC welding for tool rotation of 1000 rpm, welding speed of 9 mm/s and welding distances noted (in meters). Courtesy of Shindo *et al.* [43].

4.2 Lap joint configuration

Lap welding requires a modified tool to ensure full disruption of the interfacial oxide layers and a wider weld than butt-welding [45, 46]. A conical pin will not produce sufficient pressure at the sides of the weld, leading to lower strength. Conventional cylindrical threaded pin originally designed for butt welding will also experience problems; most importantly sheet thinning and undisrupted oxides remaining in the material [34]. Flare Triflute ™ type pin can be designed with any combination of neutral, left or right-handed flute, or ridge groves to suit the material and joint geometry being welded (see Fig. 17). Moreover, Figure 17 shows that the individual ridges on the probe can be regarded as independent features. This effectively plasticizes material and moves the fragmented oxides upward or downward as required with every 120 degree part rotation of the pin [45, 47].

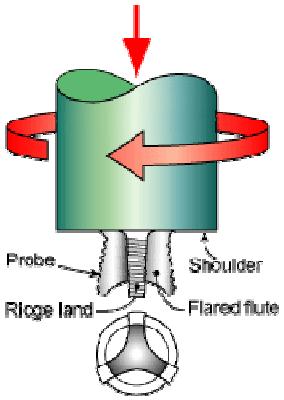

Fig. 17: Flare Triflute ™ tool.

Skew-stir variant of FSW differs from the conventional method in that the tool axis is slightly skew to the machine spindle as shown in Fig. 18. As the probe does not rotate on its own axis only a specific part of the face is directly involved in material work.

Consequently, the inner part of the pin is removed to increase the ratio between the swept material volume and the pin volume. This approach is beneficial for oxide disruption and the experimental results indicate an improvement of the tensile and fatigue properties of FSWed lap joints [22, 34, 35, 41, 45].

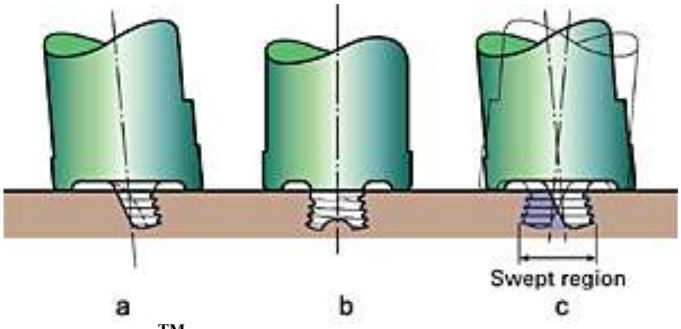

Fig. 18: A-skew ™ tool.

Conclusions

For the last fifteen years, progresses in FSW technology have been mainly related to new tool development and a better understanding of the process. The design of the tool shoulder-pin system influences significantly joint quality and reduces the loads during the process. The present review was based on an extensive literature survey on the influence of tool geometry the selection of the FSW process parameters, the interactions between the tool and the metallic sample, and the resulting properties of the joint. However, there is generally a lack of information in the literature or the public domain about FSW tools. This lack of data may be explained by the fact that the FSW process is not mature yet: FSW tools are not standardized, welding procedure standards are not developed, and the possibility that the in-house successful practices are not published and reported to the industrial and/or research community. It is hoped that initiatives, such as MTS user's group or American Welding Society committees will help to develop a strong scientific and technical basis for the design, and applications of FSW tools.

Acknowlegments

The authors thank P. Dong from Battelle, Murr. L from University of Texas, D. Hattingh from Nelson Mandela Metropolitan University, Colegrove P. and H. Shercliff from Cranfield University, Russell M. from TWI and Buffa G. from Viale delle Scienze for the agreement to use their results.

References

[1] T. Källgren, *"Friction Stir Welding of Copper Canisters for Nuclear Waste"*, PhD Thesis, Royal Institute of Technology (KTH), Stockholm, Sweden, (2005).
[2] N.G. Tretyak, Paton Welding Journal, Vol. 7 (2002) 10-18.
[3] K. Kimapong, T. Watanabe, Welding Journal, Vol. 83 (2004) 277-282.
[4] Y. Shi Qing, T. Dickerson, R. Shercliff Hugh, *"Thermo-mechanical analyses of welding aluminium alloy with TIG and friction stir welding"*, 6th International Conference: Trends in Welding Research, Pine Mountain, GA, USA, ASM International, 15-19 Apr., 2002, 247-252.
[5] T.H. North, G.J. Bendzsak, C.B. Smith, G.H. Luan, *"Numerical modeling and validation during friction stir welding of aluminium alloys"*, Today and Tomorrow in Science and Technology of Welding and Joining, Proceedings, 7th JWS International Symposium 7WS, Kobe, Tokyo, 20-22 Nov., 2001, 621-632.

[6] R.J. Lederich, J.A. Baumann, P.A. Oelgoetz, *"Friction stir welding of D357 castings and 2024 wrought products"*, Friction Stir Welding and Processing, Indianapolis, IN, USA, TMS (The Minerals, Metals & Materials Society), 4-8 Nov., 2001.
[7] R.S. Mishra, Advanced Materials & Processes, Vol. 161 (2003) 43-46.
[8] P.B. Berbon, W.H. Bingel, R.S. Mishra, C.C. Bampton, M.W. Mahoney, Scripta Materialia, Vol. 44 (2001) 61-68.
[9] I. Charit, Z.Y. Ma, R.S. Mishra, *"High strain rate superplasticity in aluminum alloys via friction stir processing"*, Advances in Superplasticity and Superplastic Forming, Charlotte, NC, USA, TMS (The Minerals, Metals & Materials Society), 14-18 Mar., 2004, 201-209.
[10] I. Charit, R.S. Mishra, Materials Science and Engineering A, Vol. 359 (2003) 209-296.
[11] T.J. Lienert, W.L. Stellwag, L.R. Lehman, *"Heat inputs, peak temperatures and process efficiencies for FSW"*, 4th International Symposium on Friction Stir Welding, Park City, UT, USA, Abington, Cambridge CB1 6AL, UK; TWI Ltd, 14-16 May, 2003, 10.
[12] P.A. Colegrove, H.R. Shercliff, Science and Technology of Welding and Joining, Vol. 9 (2004) 352-361.
[13] P. Dong, F. Lu, J.K. Hong, Z. Cao, Science and Technology of Welding and Joining, Vol. 6 (2001) 281-287.
[14] W.-S. Chang, H.-S. Bang, S.-B. Jung, Y.-M. Yeon, H.-J. Kim, W.-B. Lee, *"Joint properties and thermal behaviors of friction stir welded age hardenable 6061Al alloy"*, THERMEC 2003: International Conference on Processing & Manufacturing of Advanced Materials, Madrid, Spain, Materials Science Forum, 7-11 July, 2003, 2953-2958.
[15] O. Frigaard, O. Grong, O.T. Midling, Metallurgical and Materials Transactions A, Vol. 32 (2001) 1189-1200.
[16] T. Shinoda, Welding in the World, Vol. 47 (2003) 18-23.
[17] J.A. Wert, Scripta Materialia, Vol. 49 (2003) 607-612.
[18] Y.S. Sato, S.H.C. Park, M. Michiuchi, H. Kokawa, Scripta Materialia, Vol. 50 (2004) 1233-1236.
[19] P.A. Colegrove, H.R. Shercliff, Journal of Materials Processing Technology, Vol. 169 (2005) 320-327.
[20] J.A. Schneider, A.C. Nunes, Jr., Metallurgical and Materials Transactions B, Vol. 35B (2004) 777-783.
[21] H.N.B. Schmidt, T.L. Dickerson, J.H. Hattel, Acta Materialia, Vol. 54 (2006) 1199-1209.
[22] M. Guerra, C. Schmidt, J.C. McClure, L.E. Murr, A.C. Nunes, Materials Characterization, Vol. 49 (2002) 95-101.
[23] P. Heurtier, C. Desrayaud, F. Montheillet, Materials Science Forum, Vol. 396-402 (2002) 1537-1542.
[24] P. Heurtier, M.J. Jones, C. Desrayaud, J.H. Driver, F. Montheillet, D. Allehaux, Journal of Materials Processing Technology, Vol. 171 (2006) 348-357.
[25] L. Dubourg, F.O. Gagnon, L. St-Georges, M. Jahazi, F.G. Hamel, *"Process window optimization for FSW of thin and thick sheet Al alloys using statistical methods"*, 6th symposium of Friction stir welding, St Sauveur, QC, Canada, Oct. 10-13, 2006.
[26] K.V. Jata, Materials Science Forum, Vol. 3 (2000) 1701-1712.
[27] M.N. James, G.R. Bradley, H. Lombard, D.G. Hattingh, Fatigue and Fracture of Engineering Materials and Structures, Vol. 28 (2005) 245-256.
[28] O.T. Midling, G. Rorvik, *"Effect of tool shoulder material on heat input during friction stir welding"*, 1st International Symposium on Friction Stir Welding, Thousand Oaks, CA, USA, 14-16 June, 1999.
[29] I.H. Brown, *"Friction welding at Adelaide University"*, Challenges for Innovation in the New Millennium, WTIA 49th Annual Conference, Adelaide, Australia, Silverwater, 8-10 Oct., 2001.
[30] K.J. Colligan, P.J. Konkol, J.J. Fisher, J.R. Pickens, Welding Journal (USA), Vol. 82 (2003) 34-40.
[31] K.J. Colligan, X. Junde, J.R. Pickens, *"Welding tool and process parameter effects in friction stir welding of aluminum alloys"*, Friction Stir Welding and Processing II, San Diego, CA, USA, TMS (The Minerals, Metals & Materials Society), 2-6 March, 2003, 181-190.
[32] A.P. Reynolds, W. Tang, *"Alloy, tool geometry, and process parameter effects on friction stir weld energies and resultant FSW joint properties"*, Friction Stir Welding and Processing, Indianapolis, IN, USA, TMS (The Minerals, Metals & Materials Society)2001, 15-23.
[33] J. Lumsden, G. Pollock, M. Mahoney, *"Effect of tool design on stress corrosion resistance of FSW AA7050-T7451"*, Friction stir welding and processing III, San Francisco, CA, USA, TMS (The Minerals, Metals & Materials Society), Feb. 13-17, 2005, 19-25.

[34] M. Ericsson, *"Fatigue strength of friction stir welded joints in aluminium"*, PhD Thesis, Royal institute of Technologies, Stockholm, Sweden, (2005) 156 pages.
[35] G.M.D. Cantin, S.A. David, W.M. Thomas, E. Lara-Curzio, S.S. Babu, Science and Technology of Welding and Joining, Vol. 10 (2005) 268-280.
[36] R. Zettler, S. Lomolino, J. Dos Santos, T. Donath, F. Beckmann, T. Lippman, D. Lohwasser, *"Effect of tool geometry and process parameters on material flow in FSW of AA 2024"*, Welding and Brazing in Aerospace Industry, Berlin-Schonefeld, 12-13 May, 2004, 83-89.
[37] D.G. Hattingh, T.I. van Niekerk, C. Blignault, G. Kruger, M.N. James, Welding in the World, Vol. 48 (2004) 50-58.
[38] P.A. Colegrove, H.R. Shercliff, Science and Technology of Welding and Joining, Vol. 9 (2004) 345-351.
[39] G. Buffa, J. Hua, R. Shivpuri, L. Fratini, Materials Science and Engineering A, Vol. 419 (2006) 389-396.
[40] G. Buffa, J. Hua, R. Shivpuri, L. Fratini, Materials Science and Engineering A, Vol. 419 (2006) 381-388.
[41] J.H. Ouyang, D. Jandric, R. Kovacevic, M. Song, M. Valant, *"Visualization of material flow during friction stir welding of the same and dissimilar aluminum alloys"*, 6th International Conference: Trends in Welding Research, Pine Mountain, GA; USA, ASM International, 15-19 Apr., 2002, 229-234.
[42] W.M. Thomas, S.A. Lockyer, S.W. Kallee, D.G. Staines, *"Friction stir welding - an update on recent developments"*, Stressed Components in Aluminium Alloys, Birmingham, UK, 2 Apr., 2003.
[43] D.J. Shindo, A.R. Rivera, L.E. Murr, Journal of Materials Science, Vol. 37 (2002) 4999-5005.
[44] R.A. Prado, L.E. Murr, K.F. Soto, J.C. McClure, Materials Science and Engineering A, Vol. 349 (2003) 156-165.
[45] W.M. Thomas, K.I. Jonhson, C.S. Wiesner, Advanced Engineering Materials, Vol. 5 (2003) 485-490.
[46] M.J. Brooker, A.J. Van Deudekom, S.W. Kallee, P.D. Sketchley, *"Applying Friction Stir Welding to the Ariane 5 Main Motor Thrust Frame"*, European Conference on Spacecraft Structures, Materials and Mechanical Testing, Noordwijk, The Netherlands, European Space Agency, 29 Nov. - 1 Dec., 2000, 507.
[47] O.K. Mishina, A. Norlin, *"Lap joints produced by FSW on flat aluminium EN AW-6082 profiles"*, 4th International Symposium of Friction Stir Welding, Park City, UT, USA, Abington, Cambridge CB1 6AL, UK; TWI Ltd, 14-16 May, 2003.
[48] J. Mononen, M. Siren, H. Hanninen, Welding in the World, Vol. 47 (2003) 32-35.